



Contents lists available at ScienceDirect



Applied Catalysis A: General

journal homepage: www.elsevier.com/locate/apcata

Glycerol oxidation in liquid phase: Highly stable Pt catalysts supported on ion exchange resins

Martín S. Gross, Bárbara S. Sánchez, Carlos A. Querini*

Instituto de Investigaciones en Catalisis y Petroquímica (INCAPE) – FIQ – UNL – CONICET, Santiago del Estero 2654, Santa Fe, S3000AOJ, Argentina

ARTICLE INFO

Article history:

Received 27 December 2014

Received in revised form 14 April 2015

Accepted 18 April 2015

Available online xxx

Keywords:

Glycerol

Glyceric acid

Platinum

Ion exchange resin

ABSTRACT

The glycerol oxidation reaction in liquid phase was studied using platinum supported on ion exchange resin as catalysts, with the objective of obtaining glyceric acid. In particular, the effect of the competitor anion, which is the ion used during the support pre-treatment, was addressed. It was found that the competitor ion affects the radial distribution of the active metal in the resin sphere. As the adsorption equilibrium constant of the competitor ion increases, the penetration of platinum in the resin particle also increases. Nevertheless, this difference did not affect the catalytic performance. However, the presence of iodide as competitor ion affected the platinum chemical environment, thus modifying the platinum active sites in this catalyst. Such effect was not observed when chloride or citrate ions were used for the resin pretreatment. Therefore, the competitor ion effect on the platinum catalysts performance is related with the ion nature more than with its affinity for the resin exchange sites. Iodide is adsorbed by platinum, and consequently, it affects its electronic state improving the selectivity. These catalysts showed very good activity, and what is also very important, very good stability, being possible to maintain the conversion and selectivity for many reaction cycles.

© 2015 Elsevier B.V. All rights reserved.

1. Introduction

The growing production of biodiesel by triglycerides transesterification has generated an excess of glycerol in the world market, since approximately 100 kg of glycerol is produced for each ton of biodiesel. This led to a decrease in the price of glycerol, and in some cases it has been disposed by incineration [1–3]. Therefore, it is important to develop new applications for glycerol in order to obtain chemicals with added value, what would significantly improve the profitability of the biodiesel production process.

Glycerol is a highly functionalized molecule which could be used to obtain many useful compounds through oxidation, hydrogenolysis, dehydration, esterification, and/or polymerization [4,5]. One of the routes that have been most intensively studied over the past few years is the oxidation. Selective oxidation of glycerol leads to many valuable oxygenated compounds such as glyceric, tartronic, glycolic and hydroxypyruvic acids and dihydroxyacetone.

The oxidation products of glycerol are actually synthesized from chemical processes [6] or through low-productivity fermentation processes [7,8]. In the first method, oxidation of glycerol with

inorganic compounds (such as potassium permanganate, chromic acid or nitric acid) is a known process but it has negative effects on the environment due to the formation of undesired waste [6]. Therefore, heterogeneous catalytic oxidation of glycerol is a high potential and environmentally friendly alternative for producing these compounds of high economic value. Among them, the glyceric acid (2,3-dihydroxypropanoic acid) is widely used in medicine since it acts as glucose metabolite. It is also used as precursor for aminoacids synthesis, such as serine.

The catalytic oxidation of glycerol in liquid phase has been extensively studied in the last years, using both mono and bimetallic catalysts on different supports. The metals used in these studies included Pt [6,9–11], Au [6,12–17], Pd [6,18–21], Pt-Bi [22–25], Au-Pd [20,21,26–30] and Au-Pt [12,31] supported on carbonaceous materials (carbon black, graphite, activated carbon, carbon nanotubes) and oxides (TiO_2 , CeO_2 , Al_2O_3). It has been demonstrated that the activity and selectivity of the reaction strongly depend on the reaction conditions (temperature, pH, metal/glycerol ratio).

The pH of the reaction media plays a key role during glycerol oxidation. It is generally accepted that the presence of a base is beneficial, because higher reaction rates are obtained in this condition [11]. It has been reasonably established that in basic media, a proton is removed from the glycerol primary hydroxyl groups, as the first step of the reaction mechanism [6,9]. Nevertheless, other

* Corresponding author. Tel.: +54 342 4533858; fax: +54 342 4531068.

E-mail address: querini@fiq.unl.edu.ar (C.A. Querini).

authors have succeeded in performing the glycerol oxidation in a non-basic media. Au-Pt nanoparticles supported on H-mordenite [32], MgO [33] or carbonaceous materials [34] were found to be active for glycerol oxidation in the absence of a base. More recently, Tongsakul et al. [35] also reported that Pt and Pt-Au nanoparticles supported on hydrotalcites were able to oxidize glycerol to glyceric acid without the use of a basic medium.

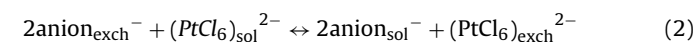
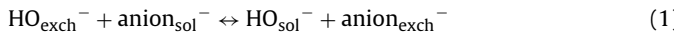
As regards the support, most authors agree that carbon-supported catalysts are more active than most oxide-supported catalysts [36,37]. Ion exchange resins offer extensive possibilities for the deposition of metals in a controlled manner both for monometallic and bimetallic catalysts. Moreover, this support has the advantage of allowing the use of fixed bed reactor configuration, which is of particular interest for the possible industrial application of the process. In addition, the ion exchange resin is highly stable in a wide range of pH. However, there is only one article in the literature in which this support was employed for the catalytic oxidation of glycerol [12].

In this work, we studied platinum catalysts supported on weak anion-exchange resin (Mitsubishi, WA-30) for the liquid phase oxidation of glycerol to obtain glyceric acid. In a previous work [38] it was reported that the concentration of the ion used during the support treatment, previous to the exchange step, affects the metal dispersion and its radial distribution along the resin particle. Such ion is known as the competitor ion, since it competes with the anion containing the active metal for the ion-exchange sites. Besides the concentration, the type of competitor anion modifies the metal distribution on the resin sphere, due to a different adsorption constant of each anion. In this work, the effect of the competitor anion as well as the reaction conditions in the catalytic performance of Pt(1%)/WA30 catalysts for glycerol oxidation reaction, was studied.

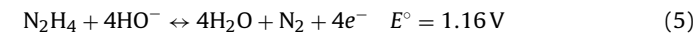
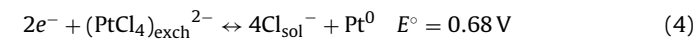
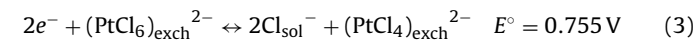
2. Experimental

2.1. Catalyst preparation

Platinum supported on ion exchange resin, prepared using hexachloroplatinic acid (H_2PtCl_6), was used as catalyst for glycerol oxidation. The resin used in this work was Mitsubishi WA-30, which is a macroporous weak anion exchange resin, with tertiary amine functional groups. The nominal platinum loading was 1 wt%, based on the mass of wet resin. The resin is provided in a basic form, i.e. with HO^- ions in the exchange sites. Before adding the metal, the resin was pretreated with different competitor anions in order to replace the hydroxyl anion. This step is represented by Eq. (1), which shows the equilibrium between the anions present in the resin ($\text{HO}_{\text{exch}}^-$) and those present in the liquid media ($\text{anion}_{\text{sol}}^-$), which are the competitor anion. It has already been reported that the type and concentration of the anion used in the pretreatment influence the radial distribution of the metal in the catalyst [38,39], this being the main reason for this step. The anions used as competitor in this study were chloride (hydrochloric acid), iodide (potassium iodide) and citrate (citric acid). The concentrations of all these solutions were 1.4 M, using one volume of solution per volume of treated resin. This concentration was chosen according to the results previously obtained when the effect of the competitor ion concentration was studied [38]. These anions incorporated into the resin, were then exchanged in a second step by the anion containing the noble metal (PtCl_6^{2-}). Before adding the solution containing the metal precursor, the resin was drained and two volumes of deionized water per volume of resin were added. Eq. (2) describes the equilibrium condition between the competitor anion in the resin and the precursor anion present in the liquid phase.



During the exchange step, that takes 30 min, it is important to maintain the system agitated to assure homogeneity in the catalyst particles. After this step, the metal was reduced with hydrazine (N_2H_4) in the presence of NaOH at a pH of 14. The reactions that take place during this step and the standard potentials of each of them are the following:



According to the potential values in Eqs. (3)–(5), it can be inferred that the reduction of platinum with hydrazine is spontaneous.

Finally, after the reduction step, the catalyst was rinsed with distilled water until neutral pH of the eluted solution.

2.2. Support and catalysts characterization

Total exchange capacity. It is the number of exchange sites present in the resin. The determination was performed using two different methods: (a) following the methodology described in ASTM D-2187 standard. This test method consists of converting the sample to the chloride form, elution of chloride with sodium nitrate, followed by determination of chloride ion in the eluted solution; (b) by titration of the resins in the HO^- form with hydrochloric acid.

Water retention capacity. It corresponds to the amount of water retained in the interstices of the polymer network. The determination was carried out following the methodology described in ASTM D-2187. It consists in the determination of the mass lost during drying at $377 \pm 2 \text{ K}$ for $18 \pm 2 \text{ h}$.

Metal loading. The metal content in the catalyst was determined by inductively coupled plasma atomic emission spectroscopy (ICP-OES) after digesting the samples with a mixture of nitric and perchloric acids. Measurements were performed with a PerkinElmer Optima 2100 DV equipment. In addition, the metal content of the aqueous solution at the end of the exchange step was also determined using the ICP technique, in order to verify the effectiveness of the ion exchange step.

Microscopic analysis. The catalysts were analyzed using optical microscopy, scanning electron microscopy (SEM), and transmission electron microscopy (TEM). The optical microscope used was a Leica, model DM2500M. The electron microscope was a JEOL JSM 35C model. The observation was made in the mode of secondary electron images using an accelerating voltage of 20 kV. Elemental chemical analyses were also carried out by X-ray, using an electron probe micro-analysis (EPMA) technique with energy-dispersive system (EDAX), attached to the scanning electron microscope. With this technique it was possible to determine the radial profile of the metal concentration in the catalyst, taking a measurement every 10 μm starting from the edge of the particle. The TEM analyses were carried out with a JEOL microscope model 100CXII operated at 100 kV. The Pt dispersion was calculated applying the equation [40]:

$$D_{\text{Pt}} = \frac{0.821}{D_{\text{va}}} \quad (6)$$

where D_{Pt} is the dispersion of platinum particles and D_{va} is a volume-area average size defined as follows:

$$D_{\text{va}} = \frac{\sum_i n_i \cdot d_i^3}{\sum_i n_i \cdot d_i^2} \quad (7)$$

being n_i the number of particles with diameter d_i .

XPS: The catalysts were analyzed by X-ray Photoelectron Spectroscopy (XPS) using a multitechnique system (SPECS), equipped with a dual Mg/Al X-ray source and a hemispherical PHOIBOS 150 analyzer operating in the fixed analyzer transmission (FAT) mode. The spectra were obtained with pass energy of 30 eV and an Al anode operated at 100 W. The pressure was maintained below 2×10^{-8} mbar during the analysis. The samples were supported on Cu double sided tape and evacuated in the prechamber for 12 h before analysis. The spectra were processed using the software Casa XPS (Casa Software Ltd., UK). The binding energy was calibrated with respect to the C1s peak (284.6 eV) of contaminated carbon.

2.3. Activity tests

Glycerol oxidation reactions were carried out in liquid phase, using a 150 mL capacity stainless steel reactor. This reactor is discontinuous in the liquid phase and continuous in the gas phase. Pure oxygen was used as oxidant, which was fed from the reactor bottom with a pressure of 150 kPa. The glycerol/metal molar ratio (GOH/M°) was varied between 700 and 1400, and the sodium hydroxide/glycerol molar ratio (NaOH/GOH) was varied between 2 and 3. Reaction temperature was varied between 303 K and 323 K. The concentration of the reactants and products were followed by high pressure liquid chromatography (HPLC), using a BioRad HPX-87H column with UV and refractive index (RI) detector. The mobile phase used was 5 mM H₂SO₄ with a flow rate of 0.6 ml min⁻¹. The products were identified and quantified by comparison with pure standards, after obtaining the calibration curves.

The conversion was determined by monitoring the glycerol concentration with time:

$$x_{\text{GOH}} = \frac{M_{\text{GOH}}^0 - M_{\text{GOH}}^t}{M_{\text{GOH}}^0} \quad (8)$$

where x_{GOH} is the glycerol conversion; M_{GOH}^0 is the glycerol initial molar concentration; M_{GOH}^t is the glycerol molar concentration at time t .

The selectivity to compound i was determined as indicated in Eq. (9):

$$S_i = \frac{M_i^t}{(M_{\text{GOH}}^0 - M_{\text{GOH}}^t)} \cdot \frac{n_i}{3} \quad (9)$$

where M_i^t is the molar concentration of compound i at time t , and n_i is the carbon atoms number of the corresponding compound.

The turn over frequency (TOF) was calculated by dividing the number of glycerol molecules consumed per unit time and per atom of platinum exposed:

$$\text{TOF} = \frac{M_{\text{GOH}}^0 \cdot (x_{\text{GOH}2} - x_{\text{GOH}1})}{C_{\text{Pt}} \cdot D_{\text{Pt}} \cdot m_{\text{cat}} \cdot (t_2 - t_1)} \quad (10)$$

where C_{Pt} is the Pt concentration in the catalyst, m_{cat} is the catalyst mass charged in the reactor and t is the time. This TOF is an average value between the reaction times t_1 and t_2 .

In order to evaluate the reproducibility of the activity tests, a set of five identical experiments was performed. The standard deviation of the conversion and selectivity to glyceric acid obtained was 0.014 and 1.214, respectively.

2.4. Catalyst stability

The catalyst stability was determined by performing 17 consecutive reaction cycles, and comparing the activity and selectivity to glyceric acid obtained in each test. Between cycles, the reaction system was rinsed with deionized water. Additionally, the chemical stability of the metal function in the catalyst was studied by

Table 1

Selectivity coefficients of anions compared to the hydroxyl ion on functionalized styrene–divinylbenzene anion exchange resins (Eq. (1)).

Competitor ion	K
Chloride	22
Iodide	175
Citrate	220

measuring the amount of Pt in the liquid phase by ICP at different times, in order to quantify the metal losses by leaching in the reaction medium. This was corroborated by measuring the metal loading in the catalyst, determined by ICP, at the start and at the end of the reaction cycles.

3. Results and discussion

3.1. Total exchange capacity and water retention capacity.

The total exchange capacity of the resin was 2.54 meq g⁻¹. This result is comparable with that reported in a previous work, in which the thermal stability of the ion exchange sites was analyzed [38]. The water retention capacity of the resin was also determined. This parameter is related to the crosslinking degree of the polymer chains; the higher the water retention capacity, the higher the crosslinking degree. The value found was 51.7%. Monitoring these parameters as the catalyst is being used in consecutive reaction cycles is useful to monitor the stability of the support. A decrease in the water retention capacity can be expected if the macropores become clogged by the impurities present in the reaction media, and/or the polymer degrades losing the crosslinking degree. Therefore, these two parameters were also determined in the catalysts used in this study. The results were similar to those found for the fresh resin, indicating that the reduced metal neither clogs the exchange sites, nor it affects the macropores volume, even after 17 cycles of reaction, as it will be shown in Section 3.4.

3.2. Catalysts preparation and characterization

Different competitor ions have been used during the catalysts preparation. In all cases, the platinum content measured by ICP, was very close to the nominal value. Moreover, the metal content of the aqueous phase obtained at the end of the exchange step (determined by ICP) was undetectable, indicating that all the platinum initially present in the liquid solution had been effectively exchanged and incorporated to the resin exchange sites. The equilibrium constants values of the exchange reaction (Eq. (1)) for different competitor ions are shown in Table 1. These values were provided by the manufacturer of the commercial resin (WA30-Mitsubishi). A larger value of the equilibrium constant indicates a major preference of the resin for this ion. Therefore, in the next step of the preparation procedure, in which the anion of the metal precursor is added to the system, it will find more resistance to replace the anions previously exchanged. As a consequence, it is expected to penetrate deeper into the resin particle. Fig. 1 shows the platinum concentration profiles for the catalysts prepared with different competitor anions, obtained using an energy-dispersive X-ray analysis (EDX) system attached to the SEM instrument. Samples have been conditioned before the analysis, by rinsing with a concentrated solution of sodium chloride, to elute the various anion exchanged after the reduction step. This operation was performed to unify the ion against which the metal was quantified, because this technique only detects elements with molecular weight higher than 23 (sodium). Assuming that all of the exchange sites were exchanged with chloride, and knowing the density of exchange sites, the metal concentration could be referred to the resin

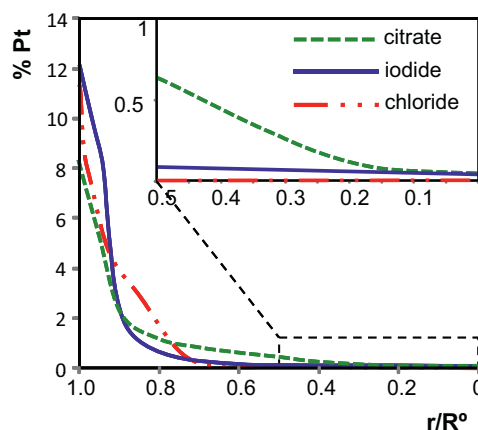


Fig. 1. Metal radial distribution in the ion exchange resin particles.

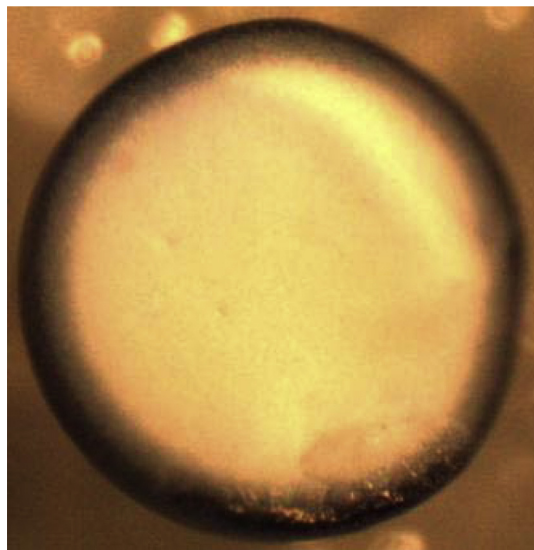


Fig. 2. Optical micrograph of a hemisphere of catalyst, prepared with iodide as competitor ion.

volume, i.e., in wt/vol% (g of Pt/100 mL of resin) through a series of calculations based on the experimental data.

Fig. 1 clearly shows that the higher the equilibrium constant, the greater the metal penetration into the resin. In the case in which chloride was used as competitor ion, the metal penetrated only 50% of the particle, while when iodide or citrate was used, the metal reached the center of the particle. The metal concentration near the particle center was slightly higher for the case in which citrate was used. For the three catalysts, a metal-rich area was observed, corresponding to a dimensionless radius (r/R°) range of approximately 1–0.9. At this distance, the metal concentration was lower than half the value of its concentration at the particle surface ($r/R^\circ = 1$). In this portion of the catalyst particle, the metal concentration was significantly higher than the nominal load, i.e., an egg-shell distribution was obtained. The metal-rich area is clearly visible, even to the naked eye. The micrograph shown in Fig. 2 was obtained using an optical microscope (Leyca DM2500M) to observe the internal surface of a catalyst particle hemisphere. The micrograph shown here corresponds to the catalyst prepared with iodide as competitor ion, but similar micrographs were obtained for the other catalysts, prepared with different competitor ions.

SEM micrographs showed that the catalysts retained the resin morphology, as shown in Fig. 3A. This observation is in agreement with the results previously discussed, i.e. the presence of 1%

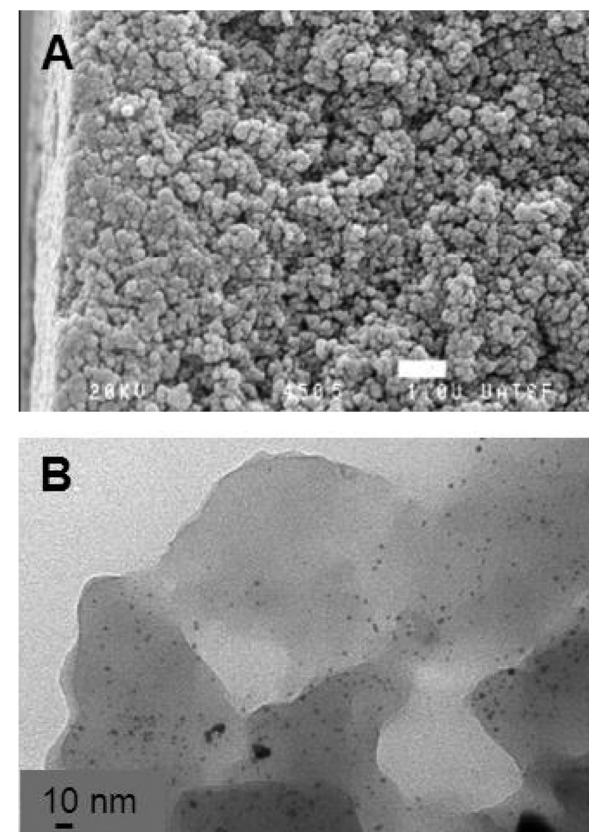


Fig. 3. (A) SEM micrograph of the catalyst border showing the characteristic resin surface; (B) TEM micrograph of the Pt particles in the resin supported catalyst.

Table 2

Average metal particle sizes, TEM particle size (D_{va}) and calculated dispersion for catalysts prepared with different competitor ions.

Competitor ion	Arithmetic mean (nm)	D_{va} (nm)	D_{Pt} (%)
Chloride	1.93	2.08	40
Iodide	1.68	1.73	48
Citrate	1.94	2.02	41

platinum in the catalyst did not alter the morphology of the support. TEM micrographs showed a very good dispersion of metallic nanoparticles in the resin, as it can be observed in Fig. 3B. Table 2 shows that similar average particle sizes were obtained when the competitor ion was chloride or citrate, but when the catalyst was prepared using iodide as competitor ion the average particle size was smaller, although the difference was only 15%. According to Fig. 4, the particle size distribution, calculated from TEM results, was narrow, with very small platinum particles of around 2 nm. Because the samples contain platinum particles of a very narrow distribution it is possible to apply equation 6 with very little error. Dispersion values of platinum particles are shown in Table 2. The three catalysts have similar values, being slightly higher for the catalyst prepared using iodide as competitor ion.

Catalyst surfaces were analyzed by XPS. Fig. 5 shows the XPS spectra obtained for catalysts pretreated with chloride and iodide in the Pt 4f region. The spectra corresponding to the catalyst pretreated with citrate were very similar to that obtained for the catalyst pretreated with chloride and hence, they are not shown in this figure. Table 3 presents the B.E. values for the Pt 4f peaks. According to these data, the Pt 4f signals of the catalysts pretreated with citrate and chloride are slightly higher than the expected for metallic Pt (71.1 eV). However, according to Ryabenkova et al. [41] the presence of small nanoparticles causes an apparent higher

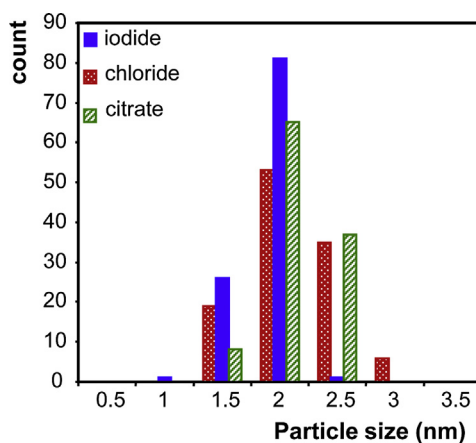


Fig. 4. Pt particle size distribution for catalysts prepared with different competitor ions.

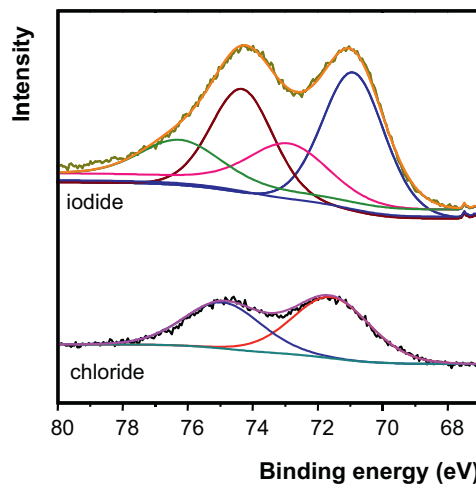


Fig. 5. XPS spectra of the iodide and chloride catalysts. Pt 4f region.

binding energy when compared with the bulk material. Therefore, the values measured for our catalysts are consistent with Pt⁰ nanoparticles. On the other hand, for the catalyst prepared with the iodide ion as competitor, the Pt 4f signal can be deconvoluted into two pairs of doublets, as shown in Fig. 5. The most intense doublet, with binding energies of 71.0 eV (Pt 4f_{7/2}) and 74.4 eV (Pt 4f_{5/2}), is assigned to metallic Pt. The other doublet, with peaks at 72.9 eV (Pt 4f_{7/2}) and 76.2 eV (Pt 4f_{5/2}) could be attributed to Pt^{δ+} [42]. According to the XPS results, 69.8% of the platinum exists as Pt⁰, whereas 30.2% is in the form of Pt^{δ+}. These are important results, and indicate that the competitor ion not only may affect the Pt distribution inside the resin particle but also its chemical state, and therefore, it can modify the catalytic performance. The reason of this difference between the catalysts prepared using iodide and chloride (or citrate) ions as competitor is not evident. However, according to studies carried out regarding the adsorption of halides

anions on the surface of Pt(111) [43] suggested that while chloride adsorption is too small, iodide forms two commensurate adlayer structures. According to Lucas et al. [43], chloride only interacts with Pt when a positive potential is applied to this metal, while iodide presents a stronger interaction, and the adsorption occurs even in the absence of an applied electrical potential. The adsorption of iodide may occur after the reduction of the (PtCl₆)²⁻, which takes place in the presence of the competitor ion that is released to the solution during the ion-exchange, as indicated in Eq. (2).

3.3. Catalytic activity tests

All the reactions were performed at a relatively low oxygen pressure (150 kPa). When higher pressures were used, it was found that glycerol over-oxidation occurred, giving products such as acetic acid, and decreasing the selectivity to glyceric acid. The oxygen pressure used for this study allows obtaining high glyceric acid yields while minimizing the formation of over-oxidized products.

Fig. 6 shows the glycerol conversion and average TOF obtained with different catalysts. Results shown in Fig. 6A correspond to the following reaction conditions: GOH/M° = 700, NaOH/GOH = 3, and T = 303 K; and in Fig. 6B the conditions were similar except that the temperature was increased to 323 K. In both figures it is observed that the catalysts prepared with chloride and citrate as competitor ions had similar activity levels. These catalysts have the same metal particle size and similar dispersion values, as was shown in Table 2, being the only difference the metal radial distribution in the polymer matrix. This indicates that the metal distribution within the catalyst particle has no significant influence on the activity thereof, and therefore it can be inferred that there are no intraparticle mass transfer limitations. The catalyst prepared with iodide as competitor had reduced activity in spite of having a metal distribution similar to that of the catalyst prepared with citrate. Moreover, the iodide catalyst is the one with the highest metal dispersion: 48% vs. 40–41% for the other catalysts (citrate, chloride). As above mentioned, iodide can be adsorbed on Pt surface, thus reducing the activity for the oxidation reaction. During the reaction in an alkaline media, additional iodide ions can be liberated from the exchange sites, by the hydroxide ions fed to the system in order to adjust the pH. Thus, these iodide ions can be further adsorbed on the Pt surface, reaction that is kinetically controlled [43], leading to faster deactivation and lower activity. This phenomena does not occur with the other competitor ions (chloride and citrate) since these ions do not adsorb on Pt, as iodide does.

Comparing Fig. 6A and B it can be seen that for all catalysts, a temperature increase led to a better conversion, although the change in activity at the end of the reaction was only 6% approximately for the catalysts prepared using chloride and citrate as competitor ions, while it was 27% in the case of using iodide as competitor ion. Also, during the 8 h of reaction, the differences in conversion and TOF between the two temperatures were always lower than expected considering only a kinetic effect according to the Arrhenius Law. It has to be taken into account that in this reaction system, the reaction in liquid phase depends both on the concentration of glycerol and oxygen. As the temperature increases, the oxygen solubility decreases, and this effect partially compensates the increase in the kinetic constant.

Fig. 7 shows the glycerol conversion and TOF curves versus time for the experiments carried out at 303 K and 323 K (Fig. 7A and B respectively); with molar ratios GOH/M° of 700, and NaOH/GOH ratio of 2. It can be seen that an increase of the reaction temperature has no significant influence on the conversion of glycerol, as also observed in the results obtained using a NaOH/GOH ratio of 3. It can also be seen that despite the conversions at 1 h reaction time are similar for the three catalysts, the TOF obtained for the catalyst pretreated with iodide is lower, since its dispersion was slightly

Table 3

Binding energies (B.E.) of the Pt 4f peaks for catalysts prepared with different competitor ions.

Competitor ion	B.E. (eV)	
	Pt 4f 5/2	Pt 4f 7/2
Chloride	74.92	71.58
Citrate	74.61	71.30
Iodide	74.4–76.2	71.0–72.9

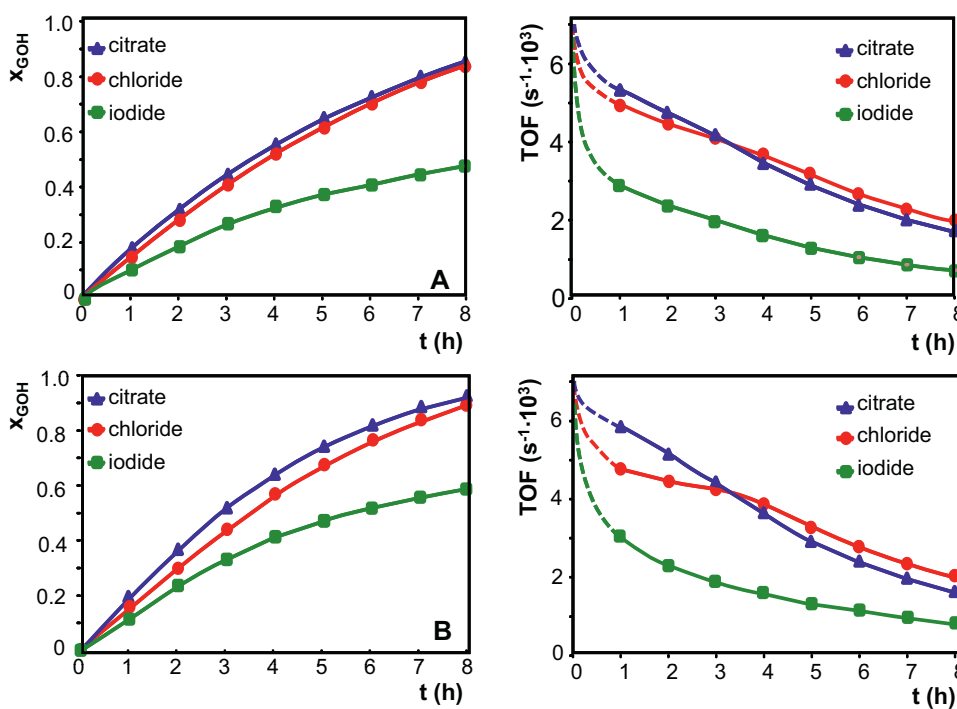


Fig. 6. Conversion curves vs time for reactions carried out at GOH/M° 700, NaOH/GOH 3, with different catalyst; (A) 303 K; (B) 323 K.

higher, as shown in Table 2. In addition, it is evident that the TOF corresponding to this catalyst considerably decreases within the first three hours of reaction. This suggests that a deactivation is taking place and it is related to the presence of iodide in the system, as above discussed.

Comparing the curves of Fig. 7A with Fig. 6A it can be inferred that decreasing the NaOH/GOH ratio has no significant influence on the activity of the catalysts prepared with chloride or citrate, since the glycerol conversion and TOF values are identical in both figures.

In the case of the catalyst prepared with iodide ion as competitor, a decrease of the NaOH/GOH ratio led to a decrease in the glycerol conversion when the reaction was carried out at 323 K. Garcia et al. [9] suggested that at a basic pH, an increment of the hydroxyls concentration (higher NaOH/GOH ratio) favors the deprotonation of the hydroxyl groups of glycerol (first step in the reaction mechanism) or the acid desorption from the metal sites (final step in the reaction mechanism), leading to an increment in the reaction rate. The initial value of TOF for the catalyst prepared with iodide was

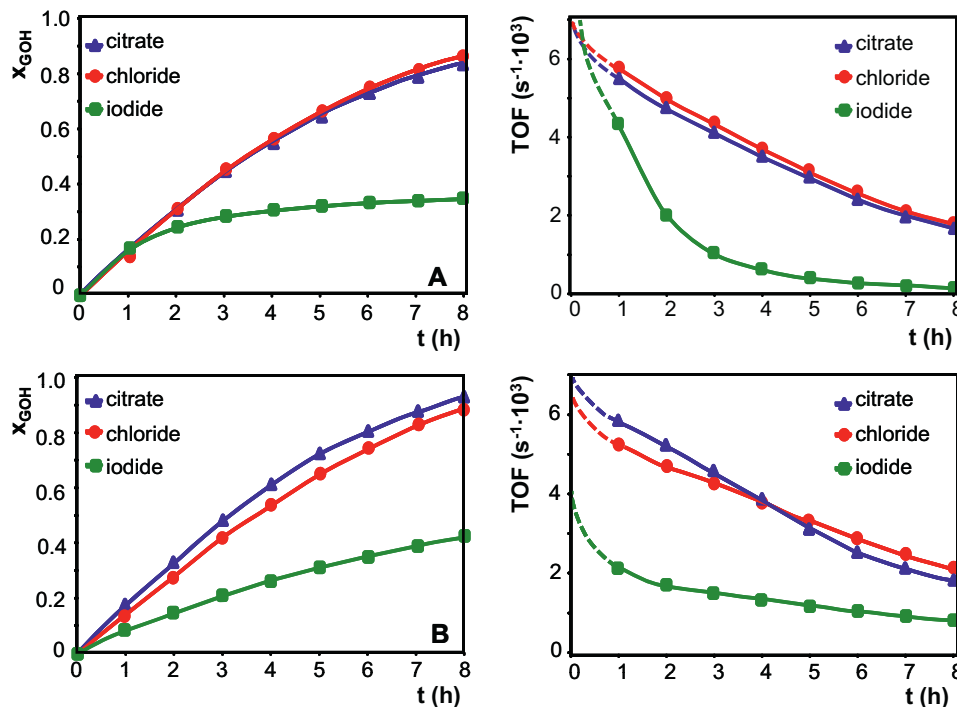


Fig. 7. Conversion curves vs time for reactions carried out at GOH/M° 700, NaOH/GOH 2, with different catalyst; (A) 303 K; (B) 323 K.

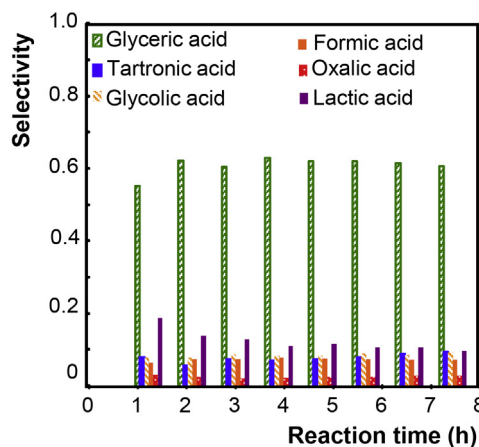


Fig. 8. Selectivity evolution with time. Reaction conditions: 323 K, GOH/NaOH 3, GOH/M° 700. Catalyst: Pt(1%) (chloride).

higher for the case where the lower ratio NaOH/GOH was used, but with the progress of the reaction these values became identical. This result can also be explained considering the effect of iodine on the platinum activity. Under oxidizing conditions, the following reaction may occur:



Iodine can also adsorb on the Pt surface, thus leading to a faster deactivation. This reaction explains the effect of the NaOH/GOH ratio. As the NaOH concentration decreases, the reaction shifts towards the products, thus increasing the concentration of iodine and consequently, the catalyst deactivation. Note that the value of the TOF (Figs. 6 and 7) as reaction time progresses decreases, indicating that the iodide-exchanged catalyst notably deactivates compared to the other catalysts.

In order to assess whether any of the reaction products is adsorbed in the ion-exchange resin, thus masking the activity results, ion exchange experiments were performed using aliquots of the liquid obtained at the end of the reaction and fresh resin. It was concluded that none of the compounds were exchanged on the exchange resin sites, since the chromatographic analysis of the liquid sample prior to contact and after 24 h contact with the resin, yielded identical concentration for all of the reaction products.

The selectivity values for different compounds remained constant during the reaction for the catalysts tested at different reaction conditions, as shown in Fig. 8 for the catalyst prepared using chloride in the pretreatment. This tendency was also observed with the other catalysts, and at different reaction conditions, i.e., in all the experiments performed the selectivity remained constant with reaction time, and thus, with the conversion. This indicates that during the reaction there were not changes on the catalyst surface, or if there were modifications such as iodine/iodide adsorption on the Pt, it only led to a change in activity. Table 4 shows the selectivity values to the different substances at the end of the reaction (8 h). It is emphasized that the selectivity remained constant throughout the reaction, i.e., it does not depend on the conversion or time, as shown in Fig. 8. For clarity reasons, the compounds are grouped according to the number of carbon atoms of the molecule. Because there is particular interest in the production of glyceric acid, substances with 3 carbon atoms are detailed, showing the selectivities to tartaric, glyceric and lactic acids. The 1C column corresponds to formic acid, which was the only 1C compound found in our experiments, while the compounds in column 2C include oxalic and glycolic acids.

Using the catalyst prepared with chloride ion as competitor, it was possible to achieve selectivity to glyceric acid of approximately

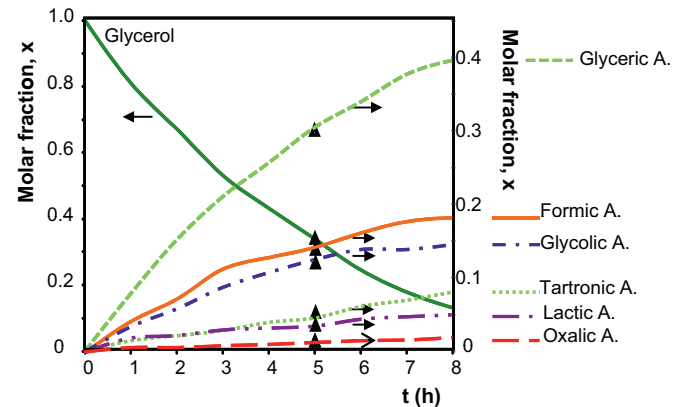


Fig. 9. Reactant liquid phase composition vs time for Pt 1% (chloride) catalyst at 303 K, NaOH/GOH ratio of 3 and GOH/M° ratio of 700; triangles: final composition obtained for the test done at the same conditions but GOH/M° ratio of 1400.

60%, at 323 K, NaOH/GOH molar ratio of 3, and not dependent on the GOH/M° ratio in the range used in this work. It can also be observed that the selectivity to compounds of 2 or 1 carbon atoms was favored with a NaOH/GOH molar ratio of 2 and low temperature (303 K). Similar results were obtained with the catalyst prepared with citrate as competitor ion: the best selectivity to glyceric acid was obtained at 323 K, NaOH/GOH ratio of 3; and the major selectivity to 1C and 2C compounds was obtained at the lowest temperature and NaOH/GOH ratio (303 K and 2 respectively). These results suggest that at lower temperature, the residence time of the intermediates compounds on the surface is longer and the coverage is higher, and therefore, the consecutive reactions occurs reaching the final step of C–C bond breaking.

The catalyst prepared with iodide ion as competitor showed selectivities to glyceric acid significantly higher than the corresponding to the other catalysts, which is related to the differences between the Pt active sites discussed in the XPS characterization section, and the possible iodide adsorption. The best selectivity values to glyceric acid were obtained at temperatures and NaOH/GOH ratios different from the other catalysts, but with the lowest GOH/M° ratio. The higher selectivity to 1C and 2C substances was observed in the experiments performed at lower temperatures and lower NaOH/GOH ratio, which is a similar result to that obtained with chloride. It was possible to obtain selectivity to glyceric acid close to 80%.

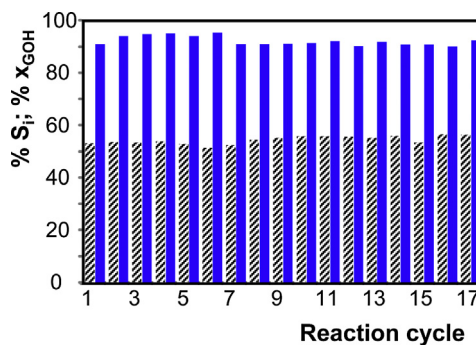
Fig. 9 shows the evolution of compositions in the reacting phase with time corresponding to an experiment performed with the catalyst prepared with chloride, at 303 K, NaOH/GOH ratio of 3 and GOH/M° ratio of 700. It is also shown in this figure the composition obtained at the end of the reaction (8 h) in the same experimental conditions, except for the GOH/M° ratio (GOH/M° of 1400). Triangles were placed at 5 h reaction time, in order to show that the reaction mechanism is not affected by the GOH/M° ratio, since almost the same product distribution (selectivity) was obtained in the two experiments at the same conversion level. Therefore, the GOH/M° ratio only influences the reaction rate, and does not affect the selectivity, being therefore possible to increase the amount of catalyst, to speed up the process, maintaining the selectivity.

3.4. Catalyst stability.

Fig. 10 shows the glyceric acid yield obtained in 17 consecutive reactions performed with the citrate treated catalyst. The results obtained reflect the remarkable stability of the platinum/resin catalysts prepared in this work, contrary to what was found in other

Table 4Conversion (x) and selectivity of Pt/resin catalysts at different reaction conditions.

Catalyst	Reaction conditions ^a	Selectivity (%)			x		
		1C ^b	2C ^c	3C			
		Tartronic	Glyceric	Lactic			
Chloride	303-3-700	8.7	15.6	11.5	56.9	7.3	0.84
	303-3-1400	9.9	14.9	6.6	62.3	6.4	0.69
	303-2-700	10.3	17.5	8.7	58.3	5.3	0.88
	303-2-1400	11.4	17.5	5.8	58.9	6.3	0.62
	323-3-700	7.4	12.4	9.6	60.8	9.8	0.89
	323-3-1400	7.5	11.3	8.3	61.8	11.1	0.62
	323-2-700	10.0	16.2	10.2	52.4	11.2	0.90
	323-2-1400	9.5	14.4	7.3	58.5	10.3	0.72
Citrate	303-3-700	7.4	12.8	12.6	61.3	5.8	0.85
	303-3-1400	9.6	15.5	7.6	60.4	7.1	0.61
	303-2-700	9.9	15.5	8.6	61.4	4.6	0.83
	303-2-1400	10.5	17.5	6.1	60.8	5.2	0.58
	323-3-700	7.8	15.0	8.2	63.0	6.1	0.91
	323-3-1400	6.6	10.3	5.9	62.1	15.1	0.44
	323-2-700	8.6	15.7	10.6	55.8	9.4	0.91
	323-2-1400	8.3	13.3	6.4	58.6	13.6	0.68
Iodide	303-3-700	6.0	6.4	5.0	78.7	3.9	0.48
	303-3-1400	6.4	6.7	5.6	75.3	5.9	0.35
	303-2-700	7.8	8.1	5.6	72.3	6.2	0.43
	303-2-1400	8.1	9.3	4.5	73.0	5.2	0.30
	323-3-700	5.4	6.4	5.4	77.5	5.3	0.59
	323-3-1400	6.5	7.2	6.8	68.5	11.1	0.58
	323-2-700	5.7	5.6	3.9	79.4	5.4	0.47
	323-2-1400	7.9	7.8	5.3	68.6	10.4	0.54

^a Temperature (K) – NaOH/GOH molar ratio – GOH/M°.^b Formic acid.^c Oxalic acid and glycolic acid.**Fig. 10.** Glyceric acid selectivity (dashed bars) and glycerol conversion (solid bars) obtained in 17 consecutive reactions. Reaction conditions: Pt 1% (citrate) catalyst, 323 K, NaOH/GOH 3, GOH/M° 700.

studies, in which it was claimed that platinum based catalysts are prone to suffer deactivation due to oxygen poisoning [44–46]. Moreover, the liquid phase was analyzed by ICP after reaction (in selected experiments), in order to quantify the possible metal losses by leaching in the reaction medium. In all cases, the platinum content was undetectable. The metal loading of the fresh catalyst, before the first reaction cycle and on the catalyst used in 17 cycles was identical and close to nominal value. Thus, it is concluded that on the prepared catalysts, the platinum function neither deactivates by oxygen poisoning, nor by leaching on the reaction medium. This is a very important result, since the catalyst stability is a key parameter in the process, being possible to reuse the catalyst in many reaction cycles.

4. Conclusions

Platinum catalysts supported on ion-exchange resins were used for the selective oxidation of glycerol. It was found that the

competitor ion used previous to the metal exchange affects the platinum penetration into the resin particle: the higher the equilibrium adsorption constant of the competitor anion, the greater the platinum penetration.

Three different competitor ions were used in this study: chloride, citrate and iodide. The catalysts prepared with chloride and citrate as competitor ions showed similar activity for the glycerol oxidation reaction in spite of their different metal distributions. On the other hand, the catalyst prepared using iodide anion as competitor, which has a similar metal distribution to that of the citrate one, showed lower activity. It is concluded that the catalytic activity is not significantly affected by the platinum distribution on the resin particle.

The reason for the different performance of the catalyst prepared by pretreating with iodide ions was attributed to the different chemical state of platinum in this catalyst, as shown by XPS. Moreover, not only the activity was affected but also the selectivity, since this catalyst showed selectivities to glyceric acid significantly higher than the corresponding to the other catalysts. This behavior is due to the iodide adsorption on Pt that modifies the electron density. According to this investigation, the nature of the competitor ion can modify the platinum active sites, thus influencing the activity and selectivity of the resin supported catalyst. It is an important finding, that the Pt modification by iodide–iodine adsorption may substantially improve the selectivity in the glycerol oxidation to glyceric acid.

Acknowledgements

The authors wish to acknowledge the financial support received from CONICET (PIP 2010-093), UNL (PACT 69) and ANPCyT (PICT 2010-1526). In addition, we thank ANPCyT for the purchase of multi-technical analysis instrument SPECS (PME8-2003).

References

- [1] X.L. Chen, Y.G. Zheng, Y.C. Shen, *Chem. Rev.* 107 (2007) 1777–1830.
- [2] J.J. Bozell, *Science* 329 (2010) 522–523.
- [3] C.H. Zhou, J.N. Beltramini, Y.X. Fan, G.Q. Lu, *Chem. Soc. Rev.* 37 (2008) 527–549.
- [4] F. Jérôme, Y. Pouilloux, J. Barrau, *ChemSusChem* 1 (2008) 586–615.
- [5] A. Corma, S. Iborra, A. Velty, *Chem. Rev.* 107 (2007) 2411–2502.
- [6] S. Carretton, P. McMorn, P. Johnston, K. Griffin, C.J. Kiely, G.J. Hutchings, *Phys. Chem. Chem. Phys.* 5 (2003) 1329–1336.
- [7] S. Varga, R. Bauer, N. Katsikis, D. Hekmat, *Chem. Eng. Technol.* 76 (2004) 1306.
- [8] H. Habe, T. Fukuoka, D. Kitamoto, K. Sakaki, *Appl. Microbiol. Biotechnol.* 84 (2009) 445–452.
- [9] R. Garcia, M. Besson, P. Gallezot, *Appl. Catal. A* 127 (1995) 165–176.
- [10] D. Liang, J. Gao, J. Wang, P. Chen, Z. Hou, X. Zheng, *Catal. Commun.* 10 (2009) 1586–1590.
- [11] D. Liang, J. Gao, H. Sun, P. Chen, Z. Hou, X. Zheng, *Appl. Catal. B* 106 (2011) 423–432.
- [12] A. Villa, C.E. Chan-Thaw, L. Pratti, *Appl. Catal. B* 96 (2010) 541–547.
- [13] P. Suramaneerat, S. Poompradub, R. Rojanathanes, P. Thamyongkit, *Catal. Lett.* 141 (2011) 1677–1684.
- [14] S. Gil, M. Marchena, L. Sánchez-Silva, A. Romero, P. Sánchez, *Chem. Eng. J.* 178 (2011) 423–435.
- [15] E.G. Rodrigues, M.F.R. Pereira, X. Chen, J.J. Delgado, J.J.M. Órfão, *J. Catal.* 281 (2011) 119–127.
- [16] E.G. Rodrigues, M.F.R. Pereira, J.J.M. Órfão, *Appl. Catal. B* 115–116 (2012) 1–6.
- [17] S. Gil, M. Marchena, C.M. Fernández, L. Sánchez-Silva, A. Romero, J.L. Valverde, *Appl. Catal. A* 450 (2013) 189–203.
- [18] N. Dimitratos, F. Porta, L. Prati, *Appl. Catal. A* 291 (2005) 210–214.
- [19] D. Wang, A. Villa, F. Porta, L. Prati, D. Su, *J. Phys. Chem. C* 112 (2008) 8617–8622.
- [20] D. Wang, A. Villa, F. Porta, D. Su, L. Prati, *Chem. Commun.* (2006) 1956–1958.
- [21] N. Dimitratos, J.A. Lopez-Sánchez, D. Lennon, F. Porta, L. Prati, A. Villa, *Catal. Lett.* 108 (2006) 147–153.
- [22] H. Kimura, K. Tsuto, T. Wakisaka, Y. Kazumi, Y. Inaya, *Appl. Catal. A* 96 (1993) 217–228.
- [23] A. Brandner, K. Lehnert, A. Bienholz, M. Lucas, P. Claus, *Top. Catal.* 52 (2009) 278–287.
- [24] N. Wörz, A. Brandner, P. Claus, *J. Phys. Chem. C* 114 (2010) 1164–1172.
- [25] W. Hu, B. Lowry, A. Varma, *Appl. Catal. B* 106 (2011) 123–132.
- [26] A. Villa, C. Campione, L. Prati, *Catal. Lett.* 115 (2007) 133–136.
- [27] L. Prati, A. Villa, C. Campione, P. Spontoni, *Top. Catal.* 44 (2007) 319–324.
- [28] W.C. Ketchie, M. Murayama, R.J. Davis, *J. Catal.* 250 (2007) 264–273.
- [29] A. Villa, D. Wang, G.M. Veith, L. Pratti, *J. Catal.* 292 (2012) 73–80.
- [30] A.A. Rodriguez, C.T. Williams, J.R. Monnier, *Appl. Catal. A* 475 (2014) 161–168.
- [31] S. Demirel, K. Lehnert, M. Lucas, P. Claus, *Appl. Catal. B* 70 (2007) 637–643.
- [32] A. Villa, G.M. Veith, L. Prati, *Angew. Chem. Int. Ed.* 49 (2010) 4499–4502.
- [33] G.L. Brett, Q. He, C. Hammond, P.J. Miedziak, N. Dimitratos, M. Sankar, A.A. Herzing, M. Conte, J.A. Lopez-Sánchez, C.J. Kiely, D.W. Knight, S.H. Taylor, G.J. Hutchings, *Angew. Chem. Int. Ed.* 50 (2011) 10136.
- [34] M. Zhang, D. Liang, R. Nie, X. Lu, P. Chen, Z. Hou, *Chin. J. Catal.* 33 (2012) 1340–1346.
- [35] D. Tongsakul, S. Nishimura, C. Thammacharoen, S. Ekgasit, K. Ebitani, *Ind. Eng. Chem. Res.* 51 (2012) 16182–16187;
- [36] D. Tongsakul, S. Nishimura, K. Ebitani, *ACS Catal.* 3 (2013) 2199–2207.
- [37] L. Prati, M. Rossi, *J. Catal.* 176 (1998) 552.
- [38] M.S. Gross, M.L. Pisarello, K.A. Pierpaoli, C.A. Querini, *Ind. Eng. Chem. Res.* 49 (2010) 81–88.
- [39] S. Oeckl, F. Martinola, P. Thomas, U.S. Patent 4,853,135 (1989).
- [40] M.S. Zanuttini, C.D. Lago, C.A. Querini, M.A. Peralta, *Catal. Today* 213 (2013) 9–17.
- [41] Y. Ryabenkova, Q. He, P.J. Miedziak, N.F. Dummer, S.H. Taylor, A.F. Carleya, D.J. Morgana, N. Dimitratos, D.J. Willocka, D. Bethell, D.W. Knight, D. Chadwickc, C.J. Kiely, G.J. Hutchings, *Catal. Today* 203 (2013) 139–145.
- [42] R. Nie, D. Liang, L. Shen, J. Gao, P. Chen, Z. Hou, *Appl. Catal. B* 127 (2012) 212–220.
- [43] C.A. Lucas, N.M. Markovic-acute, P.N. Ross, *Phys. Rev. B* 55 (1997) 7964.
- [44] L. Prati, A. Villa, C.E. Chan-Taw, R. Arrigo, D. Wang, D.S. Su, *Faraday Discuss.* 152 (2011) 353–365.
- [45] W.C. Ketchie, M. Murayama, R.J. Davis, *Top. Catal.* 44 (2007) 307–317.
- [46] C.L. Bianchi, P. Canton, N. Dimitratos, F. Porta, L. Prati, *Catal. Today* 102–103 (2005) 203–212.